

Direct Spectroscopic Characterization of Aqueous Actinyl(VI) Species: A Comparative Study of Np and U

Katharina Müller,* Harald Foerstendorf, Satoru Tsushima, Vinzenz Brendler, and Gert Bernhard

Institute of Radiochemistry, Forschungszentrum Dresden-Rossendorf e.V., P.O. Box 510119, D-01314 Dresden, Germany

Received: January 30, 2009; Revised Manuscript Received: May 5, 2009

The hydrolysis reactions of Np(VI) were investigated under an ambient atmosphere by attenuated total reflection Fourier transform infrared (ATR FT-IR) spectroscopy, NIR absorption spectroscopy, and speciation modeling applying the updated NEA thermodynamic database. For the first time, spectroscopic results of Np(VI) hydrolysis reactions are provided in the submillimolar concentration range and at pH values up to 5.3. The calculated speciation pattern and the results from FT-IR spectroscopy are comparatively discussed with results obtained from the U(VI) system under identical conditions. For both actinides, the formation of similar species can be derived from infrared spectroscopic results at pH values ≤ 4 , namely, the free cation AnO_2^{2+} (An = U, Np) and monomeric hydrolysis products. At higher pH, the infrared spectra evidence structurally different species contributing to the speciation of both actinides. At pH 5, the formation of a carbonate-containing dimeric complex, that is, $(\text{NpO}_2)_2\text{CO}_3(\text{OH})_3^-$, probably occurs during the hydrolysis reactions of neptunium, which is supported by the calculated speciation and results from NIR spectroscopy. For uranium, the presence of additional hydroxo complexes is assumed in this pH range. However, an unequivocal assignment of the spectral features to distinct species remains difficult. In particular, in the concentration range (0.5 mM) that constitutes the lower limit for the spectroscopic investigations of Np(VI) in the present work, monomeric and polymeric species obviously contribute to the U(VI) speciation considerably increasing the complexity of the spectral data.

Introduction

For the long-term storage of nuclear waste, the assessment of water contamination, depending on retention and migration processes of radionuclides in the geosphere, is of primary environmental concern. The migration behavior of (radioactive) contaminants, that is, their mobility and bioavailability in the environment, is strongly affected by molecular reactions occurring in and among solid, aqueous, and gas phases.¹ Neptunium (Np) is one of the most important actinide components of nuclear waste. Although the neptunium concentration in spent nuclear fuel is relatively low (0.03%), its concentration increases with time because of the radioactive decay of ²⁴¹Am (half-life of 432.7 years). The isotope ²³⁷Np will become a major contributor to the radiation inventory of nuclear waste repositories after about 100 000 years because of its long half-life (2.14×10^6 years).^{2,3} Therefore, in the long term safety assessment of underground disposals, great attention must be paid to its geochemistry and migration behavior.⁴ Geochemical reactions, such as complexation in solution, sorption onto mineral and biological phases, and colloids formation, are primarily defined by the oxidation state and the distribution of appropriate aqueous species of Np.^{4–6} The variety of possible oxidation states, ranging from +III to +VII is one of the peculiarities of the Np chemistry. Although, in aqueous solution, neptunium mainly occurs as the neptunyl ions NpO_2^{n+} , where $n = 1$ for Np(V) and 2 for Np(VI).⁷ The pentavalent ion dominates the Np speciation under a wide range of environmental conditions.^{8,9} However, the solution chemistry of the

hexavalent form is predicted to be relevant under oxidizing conditions of near-surface groundwater.^{10–12} The speciation of Np(VI) in aqueous solution under an ambient atmosphere is basically controlled by hydrolysis reactions and complexation with dissolved atmospheric carbon dioxide, with a strong dependence on the concentration level and pH range.^{5,13} In acidic Np(VI) solutions, the uncomplexed cation NpO_2^{2+} is known to be the predominant species. Under higher pH conditions, hydroxo and mixed hydroxo carbonate species may form.^{14,15}

Up until now, very few studies dealt with the speciation of neptunium, and most of them focused on Np(V).^{6,9,16–22} The current knowledge of thermodynamic constants of Np(VI) species is mainly based on data exclusively resulting from potentiometry and solubility measurements performed at Np(VI) concentrations in the millimolar range.^{10,14,15,23} But a structural characterization of the found species by spectroscopic techniques is still insufficient. Furthermore, modeling the commonly accepted thermodynamic data at a reduced concentration level that is adequate to environmental conditions requires extrapolation, risking inaccuracies. Therefore, a verification of the Np(VI) species at low concentrations is of urgent need for trustworthy data evaluation.

Vibrational spectroscopy and spectrophotometry are useful tools for the identification of aqueous molecular species. Regarding vibrational spectroscopy, mainly Raman studies were carried out to investigate Np(VI) hydrolysis in the past.^{24–27} However, they were restricted to Np(VI) concentrations in the millimolar range (~ 0.1 M) because of the detection limit of the applied instrumentation. Consequently, the experiments had to be performed in acidic or in carbonate solutions to avoid

* Corresponding author. Tel: ++49 351 260 2438. Fax: ++49 351 260 3553. E-mail: k.mueller@fzd.de.

precipitation of sparingly soluble neptunyl(VI) phases occurring at these concentration levels.^{24–27} This is also valid for previous investigations of the neptunium redox reactions using spectrophotometry in the near-infrared region (NIR) and the only luminescence work of Np(VI) in solution.^{28–31} Attenuated total reflection Fourier transform infrared (ATR FT-IR) spectroscopy enables the direct measurement of aqueous solutions, allowing the study at considerably reduced actinide concentrations within an extended pH range with a sufficient signal-to-noise ratio.³²

The hexavalent cations of uranium, neptunium, and plutonium exist as actinyl ions AnO_2^{2+} ($An = U, Np, Pu$) sharing the same $D_{\infty h}$ symmetry. Consequently, these metal ions show the same fundamental vibrational modes, that is, the symmetric and antisymmetric stretching vibrations denoted as ν_1 and ν_3 , respectively, and the bending vibration (ν_2).²⁴ In infrared spectroscopy, only the latter modes (ν_3 and ν_2) are observed because of the valid selection rules, but mainly the ν_3 mode serves as the characteristic spectral feature for structural analysis of the actinyl molecule complexes. In fact, the antisymmetric stretching vibrational frequencies (ν_3) of UO_2^{2+} , NpO_2^{2+} , and PuO_2^{2+} are reported to be very similar in the frequency range from 970 to 960 cm^{-1} . Therefore, vibrational spectroscopic data arising from the more thoroughly investigated U(VI) system can be valuable for the interpretation of Np(VI) and Pu(VI) data.^{24,32–34}

The aim of this study is the investigation of the Np(VI) speciation at a submillimolar concentration level in the pH range of 2–5.3 by NIR and ATR FT-IR spectroscopy and modeling thermodynamic NEA data. The obtained spectroscopic information on neptunyl complexation in aqueous solution is discussed compared with results obtained from the U(VI) system under identical conditions. Therefore, increased confidence in the thermodynamic data of both actinides might be achieved. The results obtained at a lower concentration level may be more relevant for the specific conditions occurring at radioactive waste repositories and may contribute to a more reliable safety assessment.

Experimental Section

Thermodynamic Data and Speciation Modeling. Speciation modeling of Np(VI) and U(VI) was performed using the updated thermochemical database (TDB) of the Nuclear Energy Agency (NEA).^{14,15,35} The speciation patterns were computed using the thermodynamic modeling code package EQ3/6 by Wolery.³⁶ The Davies equation was used to compute activity coefficients because none of the samples reached ionic strengths above 0.1 M.

Preparation and Characterization of Solutions. Caution! Neptunium (²³⁷Np) is a radioactive isotope and an α -emitter. It must be handled with care within laboratories appropriate for research involving transuranic elements to avoid health risks caused by radiation exposure. Highly concentrated Np solutions were handled in a reduced pressure box.

²³⁷Np dioxide was obtained from CEA-Marcoule (France). The solid was dissolved in concentrated nitric acid (65%) under stirring for several days. Then, the pH of the resulting dark brown solution was increased to about 9, and the resulting brownish precipitate was dissolved again in 1 M HCl (Merck). This procedure was repeated several times to remove nitrate ions from the Np stock solution. However, ~2% residual perchlorate arising from the Np oxide remained in the stock solution. The brownish solution was identified as 95% Np(VI) by NIR spectroscopy.⁷ A pure Np(VI) stock solution was produced electrochemically using the procedure described by

Ikeda-Ohno et al.³⁷ The radiochemical purity was checked by α/γ spectrometry using a semiconductor PIPS (PH450-21-100AM, Canberra) and a high purity germanium detector (EGM 2000-20R, Eurysis). For the U(VI) stock solution, $UO_2(NO_3)_2 \cdot 6H_2O$ (Chemapol, Czech Republic) was converted in a muffle furnace at 320 °C, and the resulting UO_3 was dissolved in 1 M HCl.³⁸

Sample preparation and analysis for the spectroscopic part of this work were done at room temperature (25 °C) under normal atmosphere. The diluted solutions of Np(VI) and U(VI) were freshly prepared using stock solutions of 0.11 M NpO_2Cl_2 and 0.05 M UO_2Cl_2 and Milli-Q water with a resistivity of 18.2 $M\Omega/cm$. Ionic strength was 0.1 M NaCl, and pH was adjusted by the addition of aliquots of 1 and 0.1 M NaOH and HCl. All reagents were of analytical grade. Chloride was used as a background electrolyte. In contrast with nitrate or perchlorate, chloride shows no absorption bands in the mid-infrared region. Ionic strength of 0.1 M is sufficiently low to avoid the formation of chloro complexes to a relevant extent.³⁹ In general, 500 μM actinide solutions were used. At this concentration level, a satisfactory signal-to-noise ratio can be achieved for the detection of aqueous Np(VI) species by applying both ATR FT-IR and NIR spectroscopy.

Liquid scintillation (Wallac Win Spectral 1414, Perkin-Elmer) and ICP-MS (ELAN 6000 Perkin-Elmer) were applied to verify the ²³⁷Np and ²³⁸U concentrations in the samples, respectively. The presence of lower oxidation states, in particular, Np(III) and Np(IV), was checked by the respective absorption bands around 786 and 960 nm in the NIR spectra, but such a situation never happened.⁷ The reduction of Np(VI) ($\lambda_{max} = 1222$ nm) to the more stable pentavalent state during the NIR measurements of Np(VI) was monitored using the absorbance of Np(V) ($\lambda_{max} = 979.5$ nm).⁷ The $Np^{VO_2^+}$ concentration in solution was calculated using the molar extinction coefficient of 395 $L mol^{-1} cm^{-1}$ at 979.5 nm and extrapolated to the total neptunium concentration in the sample. It was found that the amount of Np(V) in the solution of a pH series (pH 2.5–5.3) increases from initial 4 to 30% within 6 h of preparation and spectral analysis by NIR spectroscopy. For ATR FT-IR experiments, preparations and measurements were carried out within 1 h. Because the bands of Np(V) and Np(VI) are well separated in the optical and vibrational spectra (cf. Figures 3 and 4 and respective results section), the reduction does not significantly influence the spectral results of Np(VI) hydrolysis studies.

The check of formation of insoluble hydrolysis products was accomplished by photon correlation spectroscopy (PCS, Brookhaven Instr. 90) and ultracentrifugation. According to PCS measurements, the formation of insoluble neptunium phases could be excluded in all freshly prepared 500 μM solutions at pH values below 5.3. For the 500 μM U(VI) solutions, no precipitates were formed at $pH \leq 4.5$. The ATR-FTIR spectra of Np(VI) solutions showed no significant spectral differences before and after ultracentrifugation. (See the lower graphs of Figure A in the Supporting Information.) Moreover, one spectrum of a solution containing Np colloids was recorded for comparison. The reliability of ATR FT-IR spectroscopy to detect the formation of neptunyl(VI) colloids accurately is clearly demonstrated because the colloid spectrum shows a characteristic absorption band around 938 cm^{-1} . (See the upper graph of Figure A in the Supporting Information.) In the freshly prepared 500 μM Np(VI) solutions, this band was not found. A similar procedure to check colloids in U(VI) solutions was previously described.³²

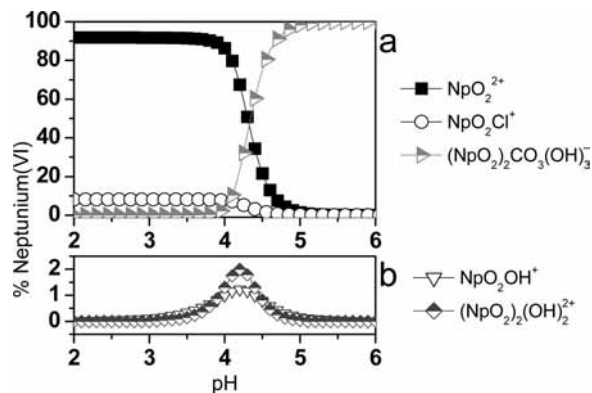


Figure 1. Speciation diagram of 500 μM Np(VI) in aqueous solution at 0.1 M NaCl under normal atmosphere. (a) Species exceeding 2% of total Np(VI) amount and (b) species <2% of total Np(VI) amount (enlarged ordinate).

Spectroscopic Studies. NIR spectra of the 500 μM Np(VI) solutions were recorded from 200 to 1400 nm in 0.1 nm interval steps using a Varian Cary 5G UV-vis-NIR spectrometer at 25 $^\circ\text{C}$. Source change was set at 350 nm and detector change was set at 900 nm. Background correction was done by subtracting spectra of respective blank solutions (0.1 M NaCl) under the same conditions as those of the Np(VI) samples.

ATR FT-IR spectra of aqueous solutions were measured on a Bruker Vertex 80/v vacuum spectrometer equipped with a mercury cadmium telluride (MCT) detector. The spectra were recorded in the range between 4000 and 400 cm^{-1} and averaged over 256 scans. Spectral resolution was 4 cm^{-1} . The used ATR unit DURA SamplIR II (Smiths), a horizontal diamond crystal with nine internal reflections on the upper surface and an angle of incidence of 45 $^\circ$, was purged with a current of dry air (dew point <213 K). The detection of the absorption of the diluted solutions requires an adequate subtraction of the background, which can satisfactorily be achieved by a thermally equilibrated acquisition system. For this purpose, a blank solution under the same conditions (pH, temperature, ionic strength) as those of the sample under investigation is rinsed with constant flow velocity of 0.2 mL/min through a flow cell mounted on the ATR crystal. Continuous acquisition of IR spectroscopic data monitors in situ the equilibration of the system. After a constant baseline is obtained, which shows very low absorption changes (optical density (OD) $\sim 10^{-4}$) in the frequency range of the water band, the respective actinyl solution with adjusted concentration is led to rinse the crystal surface. Difference spectra were calculated from spectral data recorded from the reference and the sample solution solely exhibiting those absorption changes caused by the actinyl(VI) solution. Constant parts of the spectra, in particular, the strong absorbing background from the bulk water, but also contributions from the ATR FT-IR accessory and the instrument, are eliminated. Therefore, spectral features even due to minimal absorption changes ($\sim 10^{-5}$ OD) can be detected.

Results and Discussion

Calculation of Neptunium(VI) and Uranium(VI) Speciation. The speciations of Np(VI) and U(VI) in aqueous solutions under an ambient atmosphere ($T = 25$ $^\circ\text{C}$) and at an ionic strength of 0.1 M NaCl were computed on the basis of the updated NEA TDB.^{14,15,35}

Under these conditions, the modeling of a 500 μM Np(VI) solution predicts five species in the pH range from 2 to 6 (Figure 1). The species exceeding 2% of the total Np amount are shown

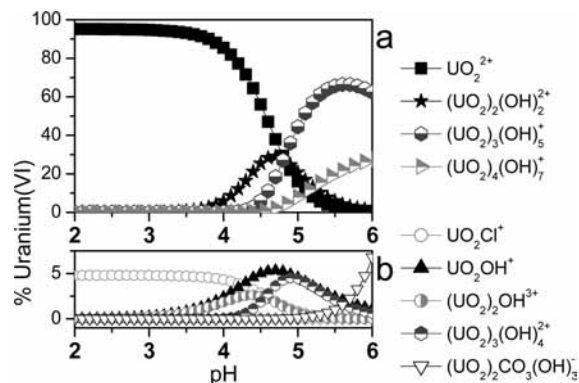


Figure 2. Speciation diagram of 500 μM U(VI) in aqueous solution at 0.1 M NaCl under normal atmosphere. (a) Species exceeding 7.5% of total U(VI) amount and (b) species <7.5% of total U(VI) amount (enlarged ordinate).

in Figure 1a, and the remaining species are shown on an enlarged scale in Figure 1b. The cation NpO_2^{2+} is calculated to dominate in acidic solution below pH 4.5, whereas the neptunyl chloride complex NpO_2Cl^+ increases to 10%. The mixed dimeric hydroxo carbonate complex $(\text{NpO}_2)_2\text{CO}_3(\text{OH})_3^-$ turns out to be the most relevant species in solution at pH > 4.5. Monomer and dimer hydroxo complexes, that is, NpO_2OH^+ and $(\text{NpO}_2)_2(\text{OH})_2^{2+}$, contribute to the Np(VI) speciation between pH 3 and 5 to only a very small amount (<2%).

The speciation pattern of aqueous U(VI) at a concentration of 500 μM in the pH range from 2 to 6 is shown in Figure 2. Again, the major species, exceeding 7.5%, are shown in Figure 2a, and the remaining species are shown on an enlarged scale in Figure 2b. The cation UO_2^{2+} predominates at pH ≤ 4.7 . In contrast with the Np(VI) system, U(VI) forms several hydrolysis complexes; in particular, the dimer $(\text{UO}_2)_2(\text{OH})_2^{2+}$ and the trimer $(\text{UO}_2)_3(\text{OH})_5^+$ govern the U(VI) speciation in the pH range of 4–6. According to the presently accepted thermodynamic data, the dimeric U(VI) mixed hydroxo carbonate complex $(\text{UO}_2)_2\text{CO}_3(\text{OH})_3^-$ becomes dominant at only pH > 6.

From these modeling efforts, it becomes evident that the speciation patterns of the two actinyl(VI) cations discussed here differ significantly. With respect to the rather similar molecular structures and effective charge distribution of both ions, this result is quite unexpected. However, one has to consider that the experimental database available to establish a set of chemical species and derive respective thermodynamic parameters is less reliable in the case of Np(VI) when compared with U(VI). This can be clearly demonstrated by a cumulative view on the related NEA TDB volumes.^{14,15,35} Namely, the Np(VI) thermodynamic data rely on only 3 and 13 original references reviewed by Lemire et al. in 2001 for the aqueous hydroxide and carbonate systems, respectively; none of them offer any structural information.¹⁵ For Np(VI) hydrolysis, only one work (Cassol et al., 1972) was integrated in the NEA data pool. The data result from acidity measurements of Np(VI) hydrolysis at concentrations in the range of 0.3–80 mM (1 M ClO_4^-) in the absence of atmospheric CO_2 .²³ Lemire et al. point out that there are no reliable data available that support thermodynamic parameters for $\text{NpO}_2(\text{OH})_2(\text{aq})$ or for neutral or anionic polymeric Np(VI) hydrolysis species, although such species may well exist.¹⁵ In the case of Np(VI) carbonate complexation, the authors suggest thermodynamic values in analogy to the better known U(VI) species with large uncertainties. They also provide maximum formation constant values rather than proposing no value at all. However, there is satisfactory experimental information avail-

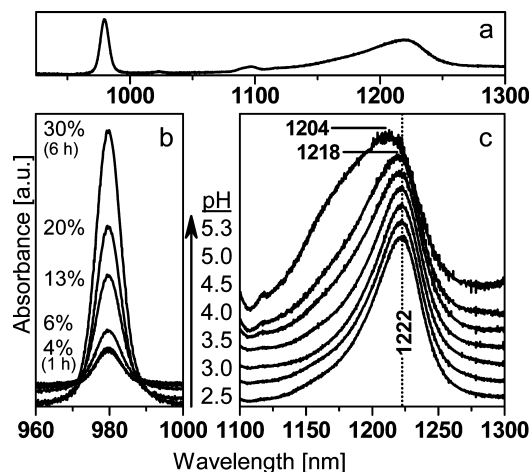


Figure 3. NIR spectra of 500 μM neptunyl(VI) solutions (0.1 M NaCl) recorded at different pH values. (a) Overview NIR spectrum at pH 5. (b) Detailed view at the absorption of the Np(V) ion. The spectra reflect the reduction of Np(VI) to Np(V) during NIR measurement time (~ 6 h). The relative amount of generated Np(V) is indicated. (c) Absorption of the Np(VI) ion at different pH values: 2.5, 3.0, 3.5, 4.0, 4.5, 5.0, and 5.3 (from bottom to top). Indicated values are in nanometers.

able for only two Np(VI) complexes in aqueous carbonate/bicarbonate media, namely, $\text{NpO}_2(\text{CO}_3)_3^{4-}$ and $(\text{NpO}_2)_3(\text{CO}_3)_6^{6-}$.¹⁵ The thermodynamic data of Np(VI) mixed hydroxo carbonate complexes result from only a few original publications and are additionally extrapolated from U(VI).¹⁰ In 2003, data of Np(VI) hydrolysis and carbonate complexation were retained in the updated NEA TDB because new data were not available.¹⁴ Concerning the U(VI) database, there are many more original data utilized in setting up both the chemical species set and their complex formation constants, with approximately 75 and 32 references for the aqueous hydroxide and carbonate systems, respectively.^{14,35} Therefore, the probability that the currently accepted set of Np(VI) hydrolysis products and carbonate complexes is incomplete, combined with inaccurate reaction constants, or both is not negligible.

Near Infrared Region Spectroscopy of Np(VI) Solutions in the Acidic pH Range. The NIR spectra of a 500 μM Np(VI) solution under varied pH conditions and an ambient atmosphere, 25 $^\circ\text{C}$, and an ionic strength of 0.1 M are shown in Figure 3. The absorption band of the NpO_2^{2+} species is observed at 1222 nm^{40,41} in the NIR spectra obtained at pH ≤ 4.0 (Figure 3c, lower traces). Upon increasing the pH, the absorption band maximum is shifted to 1218 nm at pH 4.5 and to 1204 nm at pH 5.3 (Figure 3c, upper traces). Simultaneously to the observed shift of the absorption maximum, a weak shoulder arises around 1175 nm at pH values ≥ 4.5 , showing increasing intensity with increasing pH.

Because the hexavalent neptunium is potentially reduced to the more stable $\text{Np}^{\text{V}}\text{O}_2^+$ ion under an ambient atmosphere, the spectral absorption range of the $\text{Np}^{\text{V}}\text{O}_2^+$ ion ($\lambda_{\text{max}} = 979.5$ nm) was monitored during the NIR measurements of Np(VI). The results are presented in Figure 3b, showing the intensity increase in the absorption band at 979.5 nm. It was found that the final amount of Np(V) does not exceed 30% of the total Np concentration after 6 h of measurement time. Because of strong extinction differences of the bands at 979.5 nm ($395 \text{ L mol}^{-1} \text{ cm}^{-1}$) and 1222 nm ($45 \text{ L mol}^{-1} \text{ cm}^{-1}$) for Np(V) and Np(VI), respectively,⁷ it is reasonable to show absorption changes of a few wavelengths upon the increase in pH separately and enlarged for Np(VI) in Figure 3c. However, because of the great spectral distance of the absorption bands of both neptunyl ions,

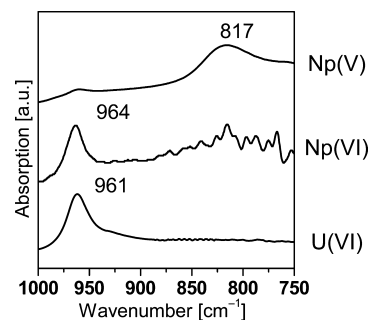


Figure 4. ATR FT-IR spectra of 100 mM Np(V), 5 mM Np(VI), and 5 mM U(VI) at pH 1.5. Indicated values are in inverse centimeters.

an interference of Np(V) species in the spectra of the Np(VI) solution shown in Figure 3a can be ruled out.

From the NIR spectra recorded at low pH values ≤ 4 , the predominance of the NpO_2^{2+} species is verified because no significant spectral alterations are observed. At pH > 4 , a change in the Np(VI) speciation can be derived by the appearance of a shoulder around 1175 nm and the observed shift of the maximum to shorter wavelengths. The small displacement of 4 nm between pH 4 and 5.3 may be due to an overlapping of absorption bands representing one or more additional species. With respect to the results of the calculated aqueous speciation of Np(VI), several species might contribute to the spectrum in the pH range > 4 (Figure 1). The species that is predicted to become predominant in the mildly acidic pH range is the dimeric $(\text{NpO}_2)_2\text{CO}_3(\text{OH})_3^-$. Therefore, the spectral alterations in the NIR spectra at $4 < \text{pH} \leq 5.3$ should mainly be due to this species. However, no structural information can be gained from the spectrophotometric measurement at least. Therefore, vibrational spectroscopy, that is, ATR FT-IR, is applied to the same solution system, first to prove the mentioned observations, and second to get structural information about the formed hydrolysis and carbonate complexed species.

Attenuated Total Reflection Fourier Transform Infrared Spectra of the Monomers of Np and U. Infrared studies of the aqueous actinyl ion speciation in the submillimolar concentration range generally reach the detection limit of conventional instrumental setups. For this reason, the spectra are expected to show a relatively low signal-to-noise ratio, which might impede an accurate evaluation of the data. Furthermore, the characteristic absorption bands of the hydrolysis products representing the ν_3 mode are expected to appear at longer wavelengths compared with those of the free monomer species. The extent of this shifting potentially provides additional information about the formed species.^{33,42} Consequently, on one hand, a detailed knowledge of the spectra of the monomeric actinyl ions will be helpful to discriminate between spectral features, which can be ascribed to residual absorptions of these ions, and randomly appearing noise. On the other hand, these spectra allow an accurate determination of the extent of the frequency shift of the ν_3 mode upon the formation of hydrolysis species, which was found to provide valuable information for spectra interpretation.

Therefore, we present the spectra of the monomeric hexavalent actinyl ions, NpO_2^{2+} and UO_2^{2+} , recorded at low pH (1.5) and at millimolar concentrations (Figure 4, lower traces). For comparison, the spectrum of the most stable neptunium species, that is, the pentavalent species NpO_2^+ , recorded under the same conditions is also shown (Figure 4, upper trace). All spectra show the absorption bands of the antisymmetric stretching vibration modes (ν_3) at 817, 964, and 961 cm^{-1} for the NpO_2^+ ,

NpO_2^{2+} , and UO_2^{2+} ions, respectively, as they were previously reported.^{26,33,34}

First, the spectra allow an unequivocal spectral distinction between the pentavalent and hexavalent state of neptunium because of the different frequencies of their absorption maxima ($\sim 150\text{ cm}^{-1}$). Complex formation of the actinyl ions in aqueous solutions, that is, hydrolysis products and carbonate complexes from dissolved atmospheric carbon dioxide, is expected to generate band shifts to lower wavenumbers up to a maximum extent of 100 cm^{-1} . From the better known U(VI) system, such shifts were reported to be from ~ 100 to $\sim 70\text{ cm}^{-1}$ for hydroxo ($\text{UO}_2(\text{OH})_4^{2-}$) and carbonate ligands ($\text{UO}_2(\text{CO}_3)_3^{4-}$), respectively.^{32,43} Therefore, when studying Np(VI) species in aqueous solution, interferences of bands from Np(V) species can be ruled out.

Second, the ν_3 modes of the hexavalent aqua ions of uranium and neptunium show very similar absorption frequencies at 961 and 964 cm^{-1} , respectively. These frequencies are in good agreement with the data obtained by authors using a dispersive IR spectrometer. Besides U(VI) and Np(VI), Jones et al. also investigated Pu(VI) and reported the ν_3 mode occurring at 962 cm^{-1} .²⁵ The deviation between the ν_3 frequencies is within 10 cm^{-1} .²⁵ This is in good agreement with results from density functional theory calculations using a scalar four-component relativistic method. From this approach, the corresponding wavenumbers were computed to be 971 , 977 , and 970 cm^{-1} for U(VI), Np(VI), and Pu(VI), respectively.⁴⁴ Because of the actinide contraction, the An– O_{ax} bond distances are slightly shortened from UO_2^{2+} over NpO_2^{2+} to PuO_2^{2+} , which shall result in an increased frequency of the ν_3 mode. However, in going from U(VI) to Np(VI) and to Pu(VI), there are increasing numbers of unpaired electron(s) which go(es) mainly into nonbonding $5f\delta$ and $5f\phi$ orbitals.⁴⁵ In the higher actinides, more electrons are localized on the metal atom; therefore, the polarization of the actinide–oxygen bond is reduced, resulting in a decreasing frequency of the ν_3 mode. Finally, these two effects mainly compensate each other, and the frequency of the ν_3 mode remains almost constant in the AnO_2^{2+} series.

With respect to the same $D_{\infty h}$ symmetry and a similar binding force constant derived from the similar frequency of the ν_3 mode of both hexavalent ions UO_2^{2+} and NpO_2^{2+} , similar spectral shifts of this mode can be expected when similar molecule complexes may occur in solution. Consequently, the hydrolysis reaction of the U(VI) system, which was extensively investigated by spectroscopic approaches in the past, can serve as a reference system for ATR FT-IR investigations of Np(VI) complexes in diluted aqueous solutions.^{32,33} Therefore, the infrared experiments were performed with both actinyl systems to obtain spectra that can be comparatively interpreted.

Attenuated Total Reflection Fourier Transform Infrared Spectroscopy of Np(VI) and U(VI) Solutions in the Acidic pH Range. The ATR FT-IR spectra obtained for $500\text{ }\mu\text{M}$ Np(VI) solutions at different pH values are shown in Figure 5a. In the region between 1300 and 1000 cm^{-1} , only one band was observed, which is due to residual perchlorate from the Np(VI) stock solution providing no relevant information. Therefore, this spectral region is not shown for clarity.

The absorption band of the ν_3 mode of the neptunyl ion is observed at 964 cm^{-1} at pH 3 (Figure 5a, upper trace). Upon increasing the pH to 4 and 4.6, a new band at 931 cm^{-1} is observed, whereas the intensity of the band at 964 cm^{-1} is considerably reduced (Figure 5a, middle traces). At pH 5.1, two overlapping bands at 943 and 931 cm^{-1} are observed (Figure 5a, lower trace). Additional spectral features are observed in

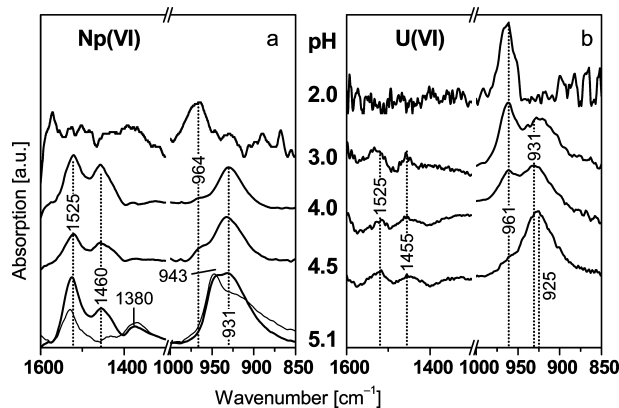


Figure 5. ATR FT-IR spectra of $500\text{ }\mu\text{M}$ oxo neptunyl(VI) and uranyl(VI) solutions at varied pH (0.1 M NaCl). (a) Spectra of Np(VI) solutions at pH 3.0, 4.0, 4.5, and 5.1 (from top to bottom). The thin line in the lower trace represents a spectrum corrected by subtraction. For details, see the text. (b) Spectra of U(VI) solutions at pH 2.0, 3.0, 4.0, and 4.5 (from top to bottom). Indicated values are in inverse centimeters.

the region between 1600 and 1300 cm^{-1} . Starting from pH 4.0, two bands are detected at 1525 and 1460 cm^{-1} , the latter showing a reduced relative intensity at higher pH (Figure 5a). Above pH 5.1, an additional band grows up at 1380 cm^{-1} (Figure 5a, lower trace).

For comparison, the obtained spectra of $500\text{ }\mu\text{M}$ U(VI) under varied pH conditions are presented in Figure 5b in the manner described above. At pH 2, a single band at 961 cm^{-1} is observed (Figure 5b, upper trace). Its intensity decreases upon increasing pH, and an additional band with absorption maximum at 931 cm^{-1} appears in the spectra at pH ≥ 3 (Figure 5b, middle traces). This band is shifted to 925 cm^{-1} in the spectrum recorded at pH value 4.5 (Figure 5b, lower trace). In analogy to the spectra of the Np(VI) solutions, additional bands at 1525 and 1455 cm^{-1} are observed at pH values ≥ 3 .

In the spectrum of the Np(VI) solution recorded at pH 3, the band at 964 cm^{-1} is assigned to the free ion NpO_2^{2+} , indicating the predominance of this species at pH ≤ 3 and at least its contribution to the speciation up to pH 4.5 (Figure 5a). In analogy, the absorption band at 961 cm^{-1} in Figure 5b is due to the free uranyl species UO_2^{2+} , strongly participating in the U(VI) speciation at pH ≤ 4.5 . The obtained spectral information agrees with the predictions from the thermodynamic data (cf. Figures 1 and 2). According to previous findings, the spectra of the uncomplexed species NpO_2^{2+} and UO_2^{2+} obviously show a reduced signal-to-noise ratio compared with the complexed species formed at a higher pH level.³² A lower absorption coefficient of the free actinyl(VI) species compared with their hydrolysis species seems to be generally characteristic.

The modeled U(VI) speciation predicts the distinct formation of hydrolysis species; that is, monomeric, dimeric, and trimeric species range between pH 4 and 6. Quilès and Burneau reported IR bands at 943 and 923 cm^{-1} in 0.1 M U(VI) solutions at pH 3.2 and 4.1 and assigned them to $(\text{UO}_2)_2(\text{OH})_2^{2+}$ and $(\text{UO}_2)_3(\text{OH})_5^+$, respectively.³³ Therefore, the U(VI) band at 931 cm^{-1} observed in this work at pH 3 and 4 (Figure 5b, middle traces) may show both species present in the $500\text{ }\mu\text{M}$ U(VI) solution in the pH range between 3 and 4. Upon further increasing the pH, the monomeric UO_2^{2+} species is hardly observed, and the fraction of the trimeric hydroxo species is obviously slightly increased, resulting in a small shift of the absorption band from 931 to 925 cm^{-1} at pH 4.5 (Figure 5b, lower trace).

From our recent work of the aqueous speciation of U(VI) at the low micromolar concentration level, another interpretation of the bands observed at $\text{pH} \geq 3$ has to be taken into account. A band at 923 cm^{-1} was observed at $\text{pH} \geq 2.5$ in a $20\text{ }\mu\text{M}$ solution and was assigned to a monomeric hydroxo complex.³² From principle thermodynamic aspects, the formation of monomeric species is more reasonable than polymeric complexes at low micromolar concentrations. However, the $500\text{ }\mu\text{M}$ concentration level used in this work might represent the concentration range of the transition from polymeric to monomeric species. Therefore, contributions of a monomer uranyl hydroxo complex in the $500\text{ }\mu\text{M}$ U(VI) solution may result in the band with absorption maximum at 925 cm^{-1} . Nevertheless, the infrared spectra shown in Figure 5b provide evidence of the formation of hydrolysis products already under lower pH conditions than those predicted by the thermodynamic data. (See Figure 2.) This is in agreement with previous results.^{32,33}

In opposition, the thermodynamic data of Np(VI) do not predict hydrolysis products contributing to the speciation to a significant extent. From the NEA database, the presence of a monomeric (NpO_2OH^+) and a dimeric species ($(\text{NpO}_2)_2(\text{OH})_2^{2+}$) can be suggested with a relative amount of $<2\%$, which is not expected to be detectable by a conventional spectroscopic technique (cf. Figure 1). The IR spectra present contradictory results, as shown in Figure 5a; at pH 4, the spectrum of the Np(VI) solution shows a strong shift of the ν_3 band to lower frequency of 33 cm^{-1} . This must be due to a drastic change in the Np(VI) speciation. A new species with absorption maximum at 931 cm^{-1} (Figure 5a) is probably formed by hydrolysis reactions at pH 4 and exists up to pH 5.1.

In contrast with the spectra of the U(VI) solutions recorded between pH 3 and 4, no significant absorption occurs around 940 cm^{-1} for the neptunyl(VI) system, which makes the formation of a dimeric hydrolysis product of Np(VI) unlikely. Therefore, the band at 931 cm^{-1} is tentatively assigned to a monomeric hydroxo species. Furthermore, this assumption is supported by the ATR FT-IR spectra presenting a speciation change at a fixed actinide-to-hydroxide ratio. (See Figure B in the Supporting Information.) Upon decreasing the Np(VI) concentration from 5 to 0.5 mM at pH 4, the two bands at 964 and 931 cm^{-1} show decreasing and increasing intensities, respectively. These spectra demonstrate that, beside the NpO_2^{2+} ion, one additional major species dominates the speciation depending on the Np(VI) concentration. Because of the decreasing concentration, this species has to be monomeric. Polymeric species can be ruled out at this pH level. Because of precipitation, millimolar concentrations cannot be investigated at higher pH without the addition of noncomplexing ligands, for example, Tetramethylammonium hydroxide (TMA-OH).

Further insight can be obtained from previous Raman spectroscopic investigations on neptunium(VI) speciation. Although the ν_1 mode of the NpO_2^{2+} cation is observed in the Raman spectra, its shift to lower wavenumbers upon hydrolysis reaction can be expected to be of the same extent as that for the ν_3 mode observed by infrared spectroscopy.³³ The symmetric stretching vibration (ν_1) of NpO_2^{2+} appears at 854 cm^{-1} in the Raman spectrum.²⁶ In an investigation of 0.1 M Np(VI) solutions in the pH range from 1.7 to 3.7, a broadening of this band was observed at pH 3.3, which was due to the presence of two bands at 854 cm^{-1} and a band, shifted about 20 cm^{-1} to lower wavenumbers, at 834 cm^{-1} , as was demonstrated by deconvolution techniques.²⁶ The shifted band was assigned to the formation of Np(VI) hydroxo complexes. According to the results of vibrational spectroscopic investigations of the hy-

drolysis reaction of U(VI), a red shift of 20 cm^{-1} of the actinyl stretching mode can be assigned to a dimeric hydroxo species.³³ Additionally, modeling of a 0.1 M Np(VI) solution based on the NEA data predicts the formation of the dimer $(\text{NpO}_2)_2(\text{OH})_2^{2+}$ at pH 3.5 to 4.2 (data not shown), which might explain the observed spectral component at 834 cm^{-1} observed in the Raman spectra of Madic et al.²⁶ However, a direct comparison of the respective Raman spectra and the IR spectra presented here is difficult because of the concentration level reduced by a factor of 200.

At $\text{pH} \geq 4.5$, the thermodynamic data of Np(VI) in $500\text{ }\mu\text{M}$ solutions predict the formation of a dimeric neptunyl mixed carbonate hydroxo complex (cf. Figure 1). The respective IR spectrum obtained at pH 5.1 exhibits an additional band at 943 cm^{-1} (Figure 5a, lower trace). In homology to the observed spectral changes discussed above, a shift of 21 cm^{-1} compared with the free neptunyl species strongly suggests the presence of a dimeric complex.^{32,33} In addition, the appearance of a band at 1380 cm^{-1} correlates with the band at 943 cm^{-1} in the spectrum recorded at pH 5.1. From the previous IR spectroscopic investigation of U(VI) in submicromolar solutions, it is assumed that the band at 1380 cm^{-1} can be ascribed to the symmetric stretching vibration of carbonate ligands complexed with a U(VI) species, for example, $\text{UO}_2(\text{CO}_3)_3^{4-}$.³² The corresponding antisymmetric stretching mode of the carbonate ligand is observed at 1525 cm^{-1} , which, in fact, shows considerably increased relative intensity in the respective spectrum (Figure 5a, lower trace). Because the pH 5.1 spectrum obviously represents contributions from two different Np(VI) species, the spectrum of the monomeric species predominating at pH 4 was subtracted. The resulting spectrum shows bands at 1529 , 1370 , and 946 cm^{-1} with a shoulder around 930 cm^{-1} representing residual contributions from the monomeric hydroxo species due to incomplete subtraction (Figure 5a, lower thin trace). The residual absorption can be eliminated by increasing the subtraction factor leading to spectral artifacts in the spectral range $>1400\text{ cm}^{-1}$. Consequently, the bands at 1375 and 1525 cm^{-1} can be assigned to the symmetric and antisymmetric stretching vibration of coordinated carbonate ligands, respectively. According to a previous study of carbonate coordination to U(VI), the splitting of these vibrational modes strongly suggests bidentate binding of the carbonate to the neptunyl(VI) ion.³² Therefore, the dominant neptunyl species at $\text{pH} > 4.5$ most probably is a carbonate containing species, for example, $(\text{NpO}_2)_2\text{CO}_3(\text{OH})_3^-$, as suggested by the thermodynamic data. (See Figure 1.)

The bands at 1525 and $\sim 1460\text{ cm}^{-1}$ appear in the spectra of both U(VI) and Np(VI) solutions when the first hydrolysis species is formed, that is, at pH 3 for U(VI) and pH 4 for Np(VI), indicating the formation of similar hydroxo complexes. However, an unequivocal assignment of these bands is difficult. One may assume that these bands are generated by a contamination with organic or inorganic ligands or by sorption processes on the used ATR crystal as well; however, this was excluded by a series of experiments in our previous study on the U(VI) speciation at low micromolar concentration level providing evidence of these spectral features as intrinsic optical absorption properties of the aqueous uranyl solutions.³² The bands possibly represent water molecules with a special coordination in the hydrate shells of the formed hydroxo complexes.

Conclusions

In the present study, we have shown that the combined approach of NIR and ATR FT-IR spectroscopy is appropriate

for studying the Np(VI) speciation in micromolar aqueous solutions. From NIR spectroscopy, information about changes in the aqueous Np(VI) speciation are obtained by slight changes of the absorption band around 1220 nm with increasing pH. The identification of different neptunyl(VI) species in solution is accomplished by ATR FT-IR spectroscopy. For the first time, the results allow the verification of current thermodynamic data by spectroscopic findings providing structural information of the aqueous Np(VI) species present at a micromolar concentration level up to pH 5.3 under distinct conditions.

The FT-IR spectra clearly demonstrate the presence of three different aqueous Np(VI) species in the acidic pH range up to pH 5.1 under an ambient atmosphere. The NpO_2^{2+} ion dominates the Np(VI) speciation below pH 3. The dimeric hydroxo carbonate complex, $(\text{NpO}_2)_2\text{CO}_3(\text{OH})_3^-$, is the most relevant species at $\text{pH} \geq 5$. These results are in good agreement with the thermodynamic data from the NEA database. In the pH range of 3–5, discrepancies between the obtained spectral information and the predicted speciation based on thermodynamic data become obvious. The ATR FT-IR spectra provide evidence of the formation of an additional hydroxo complex, most likely a monomeric hydroxo complex. In contrast, current thermodynamic data deny the presence of hydrolysis species to a relevant amount. The origin of the contradictory results might be due to the following aspects. The few Np(VI) data utilized in the NEA database to derive selected values are based on nonstructural elucidating experiments, for example, potentiometry, which were not yet verified by spectroscopic techniques providing independent structural information. Furthermore, contributions of monomeric and polymeric species to the speciation strongly depend on the neptunyl(VI) concentration. In previous spectroscopic studies, the concentrations of the investigated solutions were higher by several orders of magnitude, excluding the formation of monomeric hydroxo species.

Acknowledgment. This work was supported by the Deutsche Forschungsgemeinschaft (grant FO 619/1-1 to H.F.). We are grateful to Dr. A. Ikeda-Ohno for the help during the preparation of the Np(VI) stock solution, to C. Nebelung and U. Schaefer for α/γ and ICP-MS analysis, to K. Heim for the preparation of the U(VI) stock solution, and to S. Weiss for the PCS measurements.

Supporting Information Available: ATR FT-IR spectra of aqueous Np(VI) solutions and one Np(VI) precipitate and ATR FT-IR spectra of Np(VI) solutions at concentrations from 5 to 0.5 mM at pH 4. This material is available free of charge via the Internet at <http://pubs.acs.org>.

References and Notes

- O'Day, P. A. *Rev. Geophys.* **1999**, *37*, 249.
- Chapman, N.; Hodgkinson, D.; Maul, P. In *The Scientific and Regulatory Basis for the Geological Disposal of Radioactive Waste*; Savage, D., Ed.; Wiley: New York, 1995.
- Wilson, M. L.; Gauthier, J. H.; Barnard, R. W.; Barr, G. E.; Dockery, H. A.; Dunn, E.; Eaton, R. R.; Guerin, D. C.; Lu, N.; Martinez, M. J.; Nilson, R.; Rautman, C. A.; Robey, T. H.; Ross, B.; Ryder, E. E.; Schenker, A. R.; Shannon, S. A.; Skinner, L. H.; Halsey, W. G.; Gansemer, J. D.; Lewis, L. C.; Lamont, A. D.; Triay, I. R.; Meijer, A.; Morris, D. E. *Total-System Performance Assessment for Yucca Mountain-SNL Second Iteration*; Report SAND93-2675; Sandia National Laboratories: Albuquerque, NM, 1994.
- Kaszuba, J. P.; Runde, W. H. *Environ. Sci. Technol.* **1999**, *33*, 4427.
- Clark, D. L.; Hobart, D. E.; Neu, M. P. *Chem. Rev.* **1995**, *95*, 25.
- Neck, V.; Fanghänel, T.; Kim, J. I. *Radiochim. Acta* **1997**, *77*, 167.
- Morss, L. R.; Edelstein, N. M.; Fuger, J. *The Chemistry of the Actinide and Transactinide Elements*, 3rd ed.; Springer: Dordrecht, The Netherlands, 2006; Vol. 2.
- Nakata, K.; Fukuda, T.; Nagasaki, S.; Tanaka, S.; Suzuki, A.; Tanaka, T.; Muraoka, S. *Czech. J. Phys.* **1999**, *49*, 159.
- Rao, L. F.; Srinivasan, T. G.; Garnov, A. Y.; Zanonato, P. L.; Di Bernardo, P.; Bismondo, A. *Geochim. Cosmochim. Acta* **2004**, *68*, 4821.
- Maya, L. *Inorg. Chem.* **1984**, *23*, 3926.
- Moriyama, H.; Pratopo, M. I.; Higashi, K. *Radiochim. Acta* **1995**, *69*, 49.
- Pratopo, M. I.; Moriyama, H.; Higashi, K. *J. Nucl. Sci. Technol.* **1993**, *30*, 1024.
- Fuger, J. *Radiochim. Acta* **1992**, *58–59*, 81.
- Guillaumont, R.; Fanghänel, T.; Fuger, J.; Grenthe, I.; Neck, V.; Palmer, D. A.; Rand, M. H. *Update on the Chemical Thermodynamics of U, Np, Pu, Am, and Tc*; Elsevier: Amsterdam, 2003.
- Lemire, R. J.; Fuger, J.; Spahiu, K.; Nitsche, H.; Sullivan, J. C.; Ullman, W. J.; Potter, P.; Vitorge, P.; Rand, M. H.; Wanner, H.; Rydberg, J. *Chemical Thermodynamics of Neptunium and Plutonium*; Elsevier: Amsterdam, 2001.
- Meinrath, G. *J. Radioanal. Nucl. Chem. Lett.* **1994**, *186*, 257.
- Clark, D. L.; Conradson, S. D.; Ekberg, S. A.; Hess, N. J.; Janecky, D. R.; Neu, M. P.; Palmer, P. D.; Tait, C. D. *New J. Chem.* **1996**, *20*, 211.
- Clark, D. L.; Conradson, S. D.; Ekberg, S. A.; Hess, N. J.; Neu, M. P.; Palmer, P. D.; Runde, W.; Tait, C. D. *J. Am. Chem. Soc.* **1996**, *118*, 2089.
- Guillaume, B.; Begun, G. M.; Hahn, R. L. *Inorg. Chem.* **1982**, *21*, 1159.
- Gregoire-Kappenstein, A. C.; Moisy, P.; Cote, G.; Blanc, P. *Radiochim. Acta* **2003**, *91*, 665.
- Neck, V. *Geochim. Cosmochim. Acta* **2006**, *70*, 4551.
- Rao, L. F.; Srinivasan, T. G.; Garnov, A. Y.; Zanonato, P.; Di Bernardo, P.; Bismondo, A. *Geochim. Cosmochim. Acta* **2006**, *70*, 4556.
- Cassol, A.; Tomat, G.; Portanov., R.; Magon, L. *Inorg. Chem.* **1972**, *11*, 515.
- Basile, L. J.; Sullivan, J. C.; Ferraro, J. R.; LaBonville, P. *Appl. Spectrosc.* **1974**, *28*, 142.
- Jones, L. H.; Penneman, R. A. *J. Chem. Phys.* **1953**, *21*, 542.
- Madic, C.; Begun, G. M.; Hobart, D. E.; Hahn, R. L. *Inorg. Chem.* **1984**, *23*, 1914.
- Madic, C.; Hobart, D. E.; Begun, G. M. *Inorg. Chem.* **1983**, *22*, 1494.
- Sjoblom, R.; Hindman, J. C. *J. Am. Chem. Soc.* **1951**, *73*, 1744.
- Wester, D. W.; Sullivan, J. C. *J. Inorg. Nucl. Chem.* **1981**, *43*, 2919.
- Gelis, A. V.; Vanysek, P.; Jensen, M. P.; Nash, K. L. *Radiochim. Acta* **2001**, *89*, 565.
- Talbot-Eeckelaers, C.; Pope, S. J. A.; Hynes, A. J.; Copping, R.; Jones, C. J.; Taylor, R. J.; Faulkner, S.; Sykes, D.; Livens, F. R.; May, I. *J. Am. Chem. Soc.* **2007**, *129*, 2442.
- Müller, K.; Brendler, V.; Foerstendorf, H. *Inorg. Chem.* **2008**, *47*, 10127.
- Quilès, F.; Burneau, A. *Vib. Spectrosc.* **2000**, *23*, 231.
- Reilly, S. D.; Neu, M. P. *Inorg. Chem.* **2006**, *45*, 1839.
- Grenthe, I.; Fuger, J.; Lemire, R. J.; Muller, A. B.; Nguyen-Trung, C.; Wanner, H. *Chemical Thermodynamics of Uranium*; 1st ed.; Elsevier Science Publishers B.V.: Amsterdam, 1992.
- Wolery, T. J. *UCRL-MA-110662 Part I*. Lawrence Livermore National Laboratory: Livermore, California., 1992.
- Ikeda-Ohno, A.; Hennig, C.; Rossberg, A.; Funke, H.; Scheinost, A. C.; Bernhard, G.; Yaita, T. *Inorg. Chem.* **2008**, *47*, 8294.
- Opel, K.; Weiss, S.; Hübener, S.; Zänker, H.; Bernhard, G. *Radiochim. Acta* **2007**, *95*, 143.
- Hennig, C.; Tutschku, J.; Rossberg, A.; Bernhard, G.; Scheinost, A. C. *Inorg. Chem.* **2005**, *44*, 6655.
- Budantseva, N. A.; Fedosseev, A. M.; Bessonov, A. A.; Grigoriev, M. S.; Krupa, J. C. *Radiochim. Acta* **2000**, *88*, 291.
- Waggner, W. C. *J. Phys. Chem.* **1958**, *62*, 382.
- Nguyen-Trung, C.; Palmer, D. A.; Begun, G. M.; Peiffert, C.; Mesmer, R. E. *J. Solution Chem.* **2000**, *29*, 101.
- Lefèvre, G.; Kneppers, J.; Fédoroff, M. *J. Colloid Interface Sci.* **2008**, *327*, 15.
- Shamov, G. A.; Schreckenbach, G. *J. Phys. Chem. A* **2005**, *109*, 10961.
- Tsushima, S.; Wahlgren, U.; Grenthe, I. *J. Phys. Chem. A* **2006**, *110*, 9175.